Applied Catalysis B: Environmental 84 (2008) 148–155

Contents lists available at ScienceDirect

Applied Catalysis B: Environmental

journal homepage: www.elsevier.com/locate/apcatb

Simultaneous conversion of dye and hexavalent chromium in visible light-illuminated aqueous solution of polyoxometalate as an electron transfer catalyst

Soonhyun Kim [1], Jiman Yeo, Wonyong Choi *

School of Environmental Science and Engineering, Pohang University of Science and Technology, Pohang 790-784, Republic of Korea

ARTICLE INFO

Article history:
Received 19 November 2007
Received in revised form 16 March 2008
Accepted 20 March 2008
Available online 26 March 2008

Keywords:
Polyoxometalate
Photocatalysis
Dye
Electron transfer mediator
Visible light

ABSTRACT

This study reports the simultaneous conversion of dye and hexavalent chromium (Cr(VI)) in visible light-illuminated polyoxometalate (POM) solution. $SiW_{12}O_{40}^{4-}$ (SiW_{12}^{4-}) was used as a homogeneous catalyst that mediates the electron transfer from excited dye to heavy metal ion in the dye/Cr(VI)/POM ternary system. Rhodamine B (RhB), methylene blue (MB), and acid orange 7 (AO7) were chosen as test dyes. The conversion rate of dye and Cr(VI) in visible light-illuminated dye/Cr(VI)/POM system was strongly affected by the charge property of dye. The simultaneous conversion of cationic (RhB and MB) dye and anionic Cr(VI) were synergically enhanced in the presence of SiW_{12}^{4-}. POM successfully plays the role of the electron transfer mediator from the excited cationic dye to Cr(VI). However, the conversion of anionic dye (AO7) and Cr(VI) was negatively affected by the addition of SiW_{12}^{4-}. The observation that the initial UV/vis absorption spectrum of the dye/Cr(VI)/POM solution (with RhB or MB) was changed with increasing the concentration of SiW_{12}^{4-} indicates the complex formation between POM and cationic dyes. However, no such complex formation was observed with AO7. As for RhB, the dye degradation mechanism in the ternary RhB/Cr(VI)/POM solution was markedly different from that in the binary RhB/POM solution. The effects of various experimental parameters and the proposed mechanisms are discussed in detail.

1. Introduction

Synthetic dyes are considered one of the major aquatic pollutants because of their non-biodegradability, toxicity and unpleasant coloring. Environmental concerns about textile wastewaters that are heavily polluted with dyes call for the development of efficient and economical remediation process. Photocatalysis has been extensively investigated for the environmental pollutants degradation. Recently, polyoxometalates (POMs) have been studied as homogeneous photocatalyst and their ability to oxidize organic compounds has been demonstrated [1–3]. UV excitation of POMs induces an oxygen (ligand)-to-metal charge transfer (LMCT) with promoting an electron from the highest occupied molecular orbital (HOMO) to the lowest unoccupied molecular orbital (LUMO). The charge transfer excited state of POM (POM*) abstract an electron from substrates to yield a reduced POM (POM^-) and an oxidized substrate. POM^- can deliver the electron to various chemical species such as O_2 [4], H^+ [5], or metal ions [6,7]. POM* also may react with water to generate OH radical. Such an operating mechanism of POM photocatalyst is similarly compared with its heterogeneous counterpart, TiO_2 [2,3]. The POM/UV process has been successfully applied to dye degradation as well. Kim et al. reported that anionic AO7 dye was degraded in UV-illuminated POM solution and its degradation was completely inhibited in the presence of *tert*-butyl alcohol, an OH radical scavenger [3]. Hu and Xu also studied the photocatalytic degradation of textile dye X3B by POMs [8]. On the other hand, UV-illuminated POMs can reductively convert heavy metals such as $Cu(II) \rightarrow Cu^0$ [9], $Hg(II) \rightarrow Hg^0$ [10], and Cr(VI) → Cr(III) [11] in the presence of organic substrate as an electron donor.

Both POMs and TiO_2, which are homogeneous and heterogeneous photocatalyst, respectively, are inactive under visible light irradiation. As for the dye degradation with TiO_2, however, the visible light-induced reaction is enabled by the dye-sensitization process, which has been extensively investigated and reported in the literature [12–16]. A similar dye-sensitization process was recently demonstrated for the POM/dye system as well: excited dye injects an

* Corresponding author. Tel.: +82 54 279 2283; fax: +82 54 279 8299.
E-mail address: wchoi@postech.ac.kr (W. Choi).
[1] Current address: Division of Nano-Bio Technology, Daegu Gyeongbuk Institute of Science and Technology (DGIST), Samsung Financial Plaza, Duksan-dong 110, Jung-gu, Daegu, Republic of Korea.

0926-3373/$ – see front matter
doi:10.1016/j.apcatb.2008.03.012

electron to LUMO of POM to be oxidized [17]. The role of POM LUMO is similarly compared with that of TiO_2 conduction band in this respect. Kyung et al. demonstrated that the simultaneous conversion of dye and heavy metal ions was synergistically enhanced in the visible light-illuminated TiO_2 suspension because the electron injected from the excited dye was transferred to heavy metal ions through TiO_2 [18]. In a similar context, we may expect that the photosensitized degradation of dye can be enhanced in the presence of heavy metal ions in visible light-illuminated POM solution. Scheme 1 illustrates the proposed process. In this study, we investigated the simultaneous photoconversion of dye and heavy metal ion in the ternary dye/POM/Cr(VI) system. As illustrated in Scheme 1, the proposal that the conversion of both dye and heavy metal ion can be synergistically enhanced under visible light through the mediation of POM was successfully demonstrated.

2. Experimental

2.1. Chemicals and materials

Rhodamine B (RhB, Aldrich, 80%), Methylene blue (MB, Aldrich, 80%), Acid orange 7 (AO7, Aldrich, 87%), and $Na_2Cr_2O_7$ (Cr(VI), Aldrich) were used as received. $H_4SiW_{12}O_{40}$ (Fluka) (abbreviated as SiW_{12}^{4-}) was used as a homogeneous POM photocatalyst.

absorption peaks were at λ = 554 nm for RhB, 663 nm for MB, and 485 nm for AO7, respectively. The sample solutions may contain some fine particulate aggregates that were *in situ* formed during the irradiation of the ternary mixture and the dye absorbance was measured without filtering them. The aggregate formation was negligibly small with $[SiW_{12}^{4-}]$ = 2 μM (in most irradiation experiments). The fluorescence spectra of dyes were also obtained during the photochemical reaction using a spectrofluorometer (Shimadzu RF-5301). Excitation wavelength used was 355 nm. The conversion of Cr(VI) was monitored using an ion chromatograph (IC, Dionex DX-120) which was equipped with a Dionex IonPac AS 14 (4 mm $\times$ 250 mm) column and a conductivity detector. The eluent solution was 3.5 mM Na_2CO_3/1 mM $NaHCO_3$.

The concentration of photogenerated H_2O_2 was measured by DMP (2,9-dimethyl-1,10-phenanthroline) method [19]. The change of Cr oxidation state after the photoconversion was determined by X-ray photoelectron spectroscopy (XPS) (ESCALAB 220iXL) using the Mg Kα line (1253.6 eV) as the excitation source. The binding energies of Cr peaks were referenced to the Au $4p_{7/2}$ line (84.0 eV) from gold powder that was mixed with the collected particulate aggregate sample and checked against the C 1s line (284.6 eV) originating from surface impurity carbons.

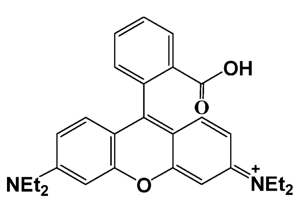
Rhodamine B

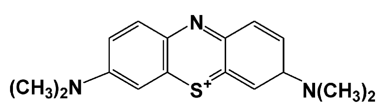
Methylene blue (MB)

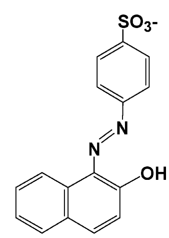
AO7

2.2. Photochemical experiments

An aliquot of RhB, MB or AO7 stock solution was added to an aqueous POM (SiW_{12}^{4-}) solution and then the heavy metal ion reagent of $Na_2Cr_2O_7$ was subsequently added to give desired initial concentrations. The total solution volume in a photoreactor was 30 mL for all cases. The pH of solutions was adjusted to 3.0 with $HClO_4$ or NaOH standard solution. The solutions were equilibrated in the dark for 30 min prior to illumination and were stirred magnetically throughout the photolysis. Photoirradiation employed a 300-W Xe arc lamp (Oriel) as a light source. Light passed through a 10-cm IR water filter and a UV cut-off filter ($\lambda > 420$ nm), then the filtered light was focused onto a 30-mL Pyrex reactor with a quartz window. The reaction temperature during irradiation was maintained below 40 °C. The reactor was filled with minimized headspace. For the N_2-saturated system, the reactor was purged with N_2 gas continuously before and during the illumination. Sample aliquots were withdrawn from the reactor intermittently during the illumination. Multiple photolysis experiments were performed under the identical reaction condition to confirm the reproducibility. The incident light intensity was measured using a power meter (Newport 1830-C). The light intensity of 420 nm cut-off filtered irradiation (I_{vis}) was measured to be 340 mW/cm^2 ($\lambda > 420$ nm).

2.3. Analyses

The removal of RhB, MB, and AO7 color was monitored using a UV/vis spectrophotometer (Agilent 8453). The monitored

3. Results and discussion

3.1. Simultaneous conversion of dye and Cr(VI)

Fig. 1 compares the simultaneous dye degradation and Cr(VI) reduction in the presence or absence of SiW_{12}^{4-}. The direct photolysis of RhB and MB was negligible and Cr(VI) was not reduced at all by SiW_{12}^{4-} alone. Although chromate is a strong oxidant, it did not oxidize the dye at all in the present experimental condition as shown in the dark control test. In the binary dye/Cr(VI) solution, the visible light-induced conversion was observed. The direct photo-induced electron transfer (from dye to Cr(VI)) in the absence of POM is possible but the conversion was highly accelerated in the presence of POM as an electron transfer catalyst. In another binary solution of dye/POM, on the other hand, RhB (or MB) can be degraded by the sensitized path [17], but the degradation rate was significantly enhanced in the presence of Cr(VI). The ternary dye/Cr(VI)/POM system showed the marked synergic effect in the conversion of both dye and Cr(VI) in comparison with the binary dye/Cr(VI) and dye/POM systems. Since POM is inactive to visible light, the highly synergic conversion observed in the ternary solution should be related with the role of POM as an electron transfer mediator from dye to Cr(VI). The excited dye transfers an electron to POM and the resulting POM^- subsequently reacts with Cr(VI) (reactions (1) and (2)) as illustrated in Scheme 1. When Cr(VI) acts as an electron acceptor in the ternary system, the dye degradation is enhanced through retarding the

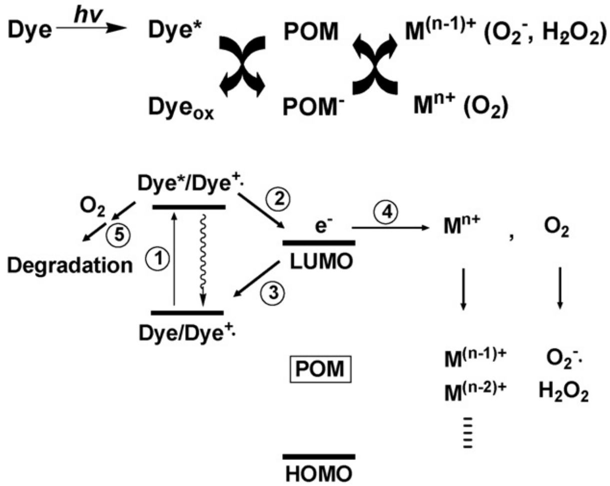

Scheme 1. Schematic illustrations of the simultaneous oxidation of dyes and reduction of metal ions (M^{n+}) in the visible light-illuminated POM solution. The upper and lower diagrams depict the photo-induced electron transfer paths from dyes to metal ions. The numbers represent main elementary paths: 1, dye excitation by visible light; 2, electron injection from the excited dye to POM LUMO; 3, back electron transfer to the oxidized dye; 4, reduction of metal ions; 5, degradation of dye through thermal radical reactions.

recombination (step 3 in Scheme 1).

$$3SiW_{12}^{5-} + HCrO_4^- + 7H^+ \rightarrow 3SiW_{12}^{4-} + Cr^{3+} + 4H_2O \quad (1)$$

$$6SiW_{12}^{5-} + Cr_2O_7^{2-} + 14H^+ \rightarrow 6SiW_{12}^{4-} + 2Cr^{3+} + 7H_2O \quad (2)$$

This is similarly compared with the simultaneous conversion of dye and Cr(VI) in the ternary dye/Cr(VI)/TiO_2 system [18], where TiO_2 acts as an electron transfer mediator from the excited dye to Cr(VI). The oxidative degradation of dyes in this ternary system, however, was not complete at all because the total organic carbon (TOC) was little removed after the irradiation. A similar study reported that the mineralization of dye in the visible-illuminated RhB/POM was negligible whereas a significant fraction of TOC could be removed (46% reduction in 20 h) in the visible-illuminated RhB/TiO_2 suspension [17]. The observed dye discoloration in the ternary dye/Cr(VI)/POM system should be induced by the selective destruction of chromophoric groups without achieving the total mineralization of the dye.

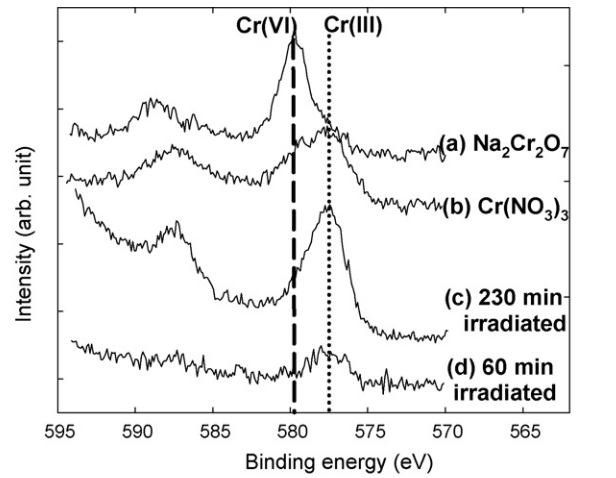

Fig. 2. X-ray photoelectron spectra of chromium (Cr 2p) species in the *in situ* generated particulate aggregate. The photoconversion condition was air-equilibrated, pH_i 3.0, $[RhB]_0 = 20\ \mu M$, $[Cr_2O_7^{2-}]_0 = 100\ \mu M$, and $[SiW_{12}^{4-}]_0 = 20\ \mu M$.

The reductive conversion of Cr(VI) and the change of the oxidation state were monitored by XPS. The visible light-induced

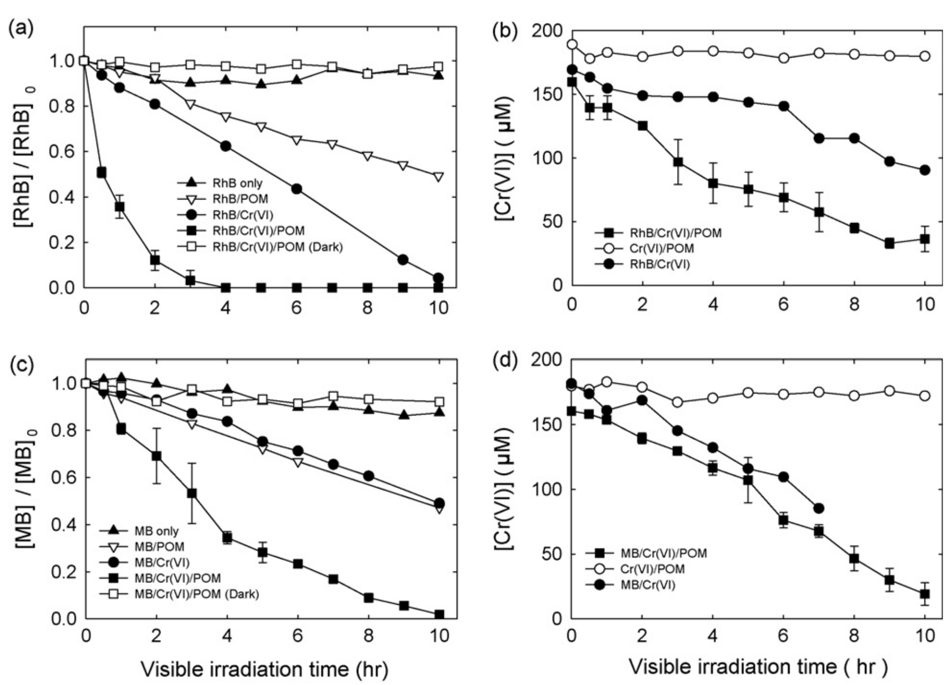

Fig. 1. Simultaneous conversion of dye and Cr(VI) in the presence or absence of POM (SiW_{12}^{4-}) under visible illumination: (a) RhB and (b) Cr(VI) in RhB/Cr(VI)/POM system ($[RhB]_0 = 20\ \mu M$, $[Cr_2O_7^{2-}]_0 = 100\ \mu M$, $[SiW_{12}^{4-}]_0 = 2\ \mu M$), (c) MB and (d) Cr(VI) in MB/Cr(VI)/POM system ($[MB]_0 = 50\ \mu M$, $[Cr_2O_7^{2-}]_0 = 100\ \mu M$, $[SiW_{12}^{4-}]_0 = 5\ \mu M$). The experimental condition was air-equilibrated, pH_i 3.0, and $\lambda > 420$ nm.

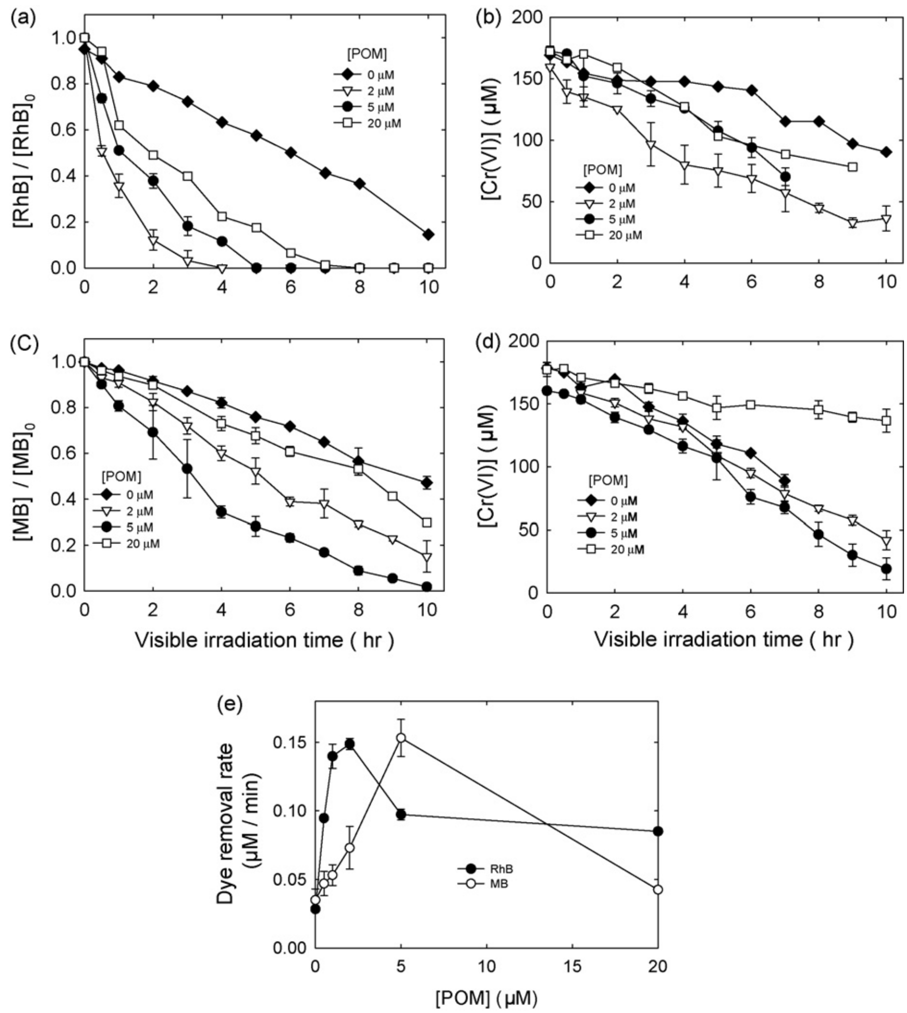

Fig. 3. Effect of SiW_{12}^{4-} concentration on the removal of (a) RhB, (b) Cr(VI) in RhB/Cr(VI)/POM, and (c) MB, (d) Cr(VI) in MB/Cr(VI)/POM, and (e) the initial removal rates (0–2 h) of dyes under visible illumination. The experimental condition was air-equilibrated, pH_i 3.0, $[RhB]_0 = 20\ \mu M$, $[MB]_0 = 50\ \mu M$, $[Cr_2O_7^{2-}]_0 = 100\ \mu M$, and $\lambda > 420$ nm.

conversion of the ternary mixture was carried out with higher [POM] (20 μM). In such condition, some fine particulate aggregates were formed during irradiation and could be filtered out from the solution. Fig. 2 shows the XPS spectra of the filtrate along with the reference spectra of Cr(VI) (i.e., $Na_2Cr_2O_7$) and Cr(III) (i.e., $Cr(NO_3)_3$). The chromium in the *in situ* formed product is clearly present as Cr(III), which confirmed that Cr(VI) was reductively converted in the ternary system.

3.2. Effect of POM concentration and POM–dye interaction

Fig. 3 shows the effect of POM concentration on the conversion of dye and Cr(VI) in the ternary (dye/Cr(VI)/POM) system under visible light. The dye removal rate increased with increasing [POM] up to 2–5 μM beyond which the rate decreased. The Cr(VI) conversion rate in the ternary system showed the similar dependence on [POM]. RhB and MB are cationic and should favorably interact with anionic POM. As a result of the electrostatic interaction, the dye degradation rate increased with [POM] although POM cannot be excited by visible light. The dye–POM interaction is spectrophotometrically supported by the spectra of Fig. 4 which shows that the dye absorption band is changed as the added POM concentration increases. The fact that excess POM retarded the conversion rate of both dye and Cr(VI) implies that the electron transfer from dye to Cr(VI) is hindered at higher [POM]. Note that the optimum concentration ratio of dye to POM is about 10:1 for both RhB and MB. The same optimal ratio ([dye]:[POM] = 10:1) was also confirmed when [RhB] = 100 μM (data not shown). Fig. 4 shows that the UV–vis absorption spectra of dye/Cr(VI)/POM solution are markedly changed when [POM] increases above this ratio. The critical POM concentration above which the dye spectral change (decreasing the main band intensity and broadening to longer wavelengths) occurs in the ternary solution roughly coincides with the POM concentration above which the dye degradation rate was reduced (see Fig. 3e). The presence of excess POM seems to induce the formation of dye–POM complex aggregates, which changes the dye spectral band. When the dye–POM complex aggregate is formed, the photoconversion efficiency may be reduced probably because the recombination rate (step 3 in Scheme 1) is accelerated within the complex. The electrons transferred from the excited dye to POM seem to immediately recombine back with the oxidized dyes instead of reacting with Cr(VI) under this condition.

As for AO7 (anionic dye), however, such complex formation was not observed (see Fig. 4c) because of the anion–anion repulsion. As a result of the different charge property of the dye, the degradation

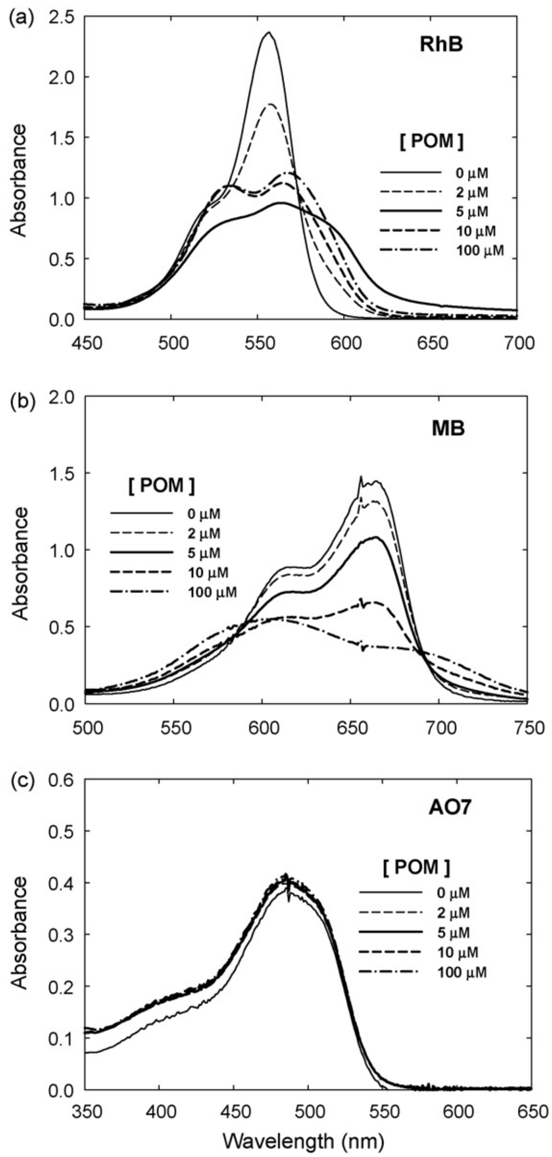

Fig. 4. Effect of SiW_{12}^{4-} concentration on the UV–vis absorption spectra of (a) RhB/Cr(VI)/POM, (b) MB/Cr(VI)/POM, and (c) AO7/Cr(VI)/POM solution. The experimental condition was air-equilibrated, pH_i 3.0, $[RhB]_0 = 20\ \mu M$, $[MB]_0 = 50\ \mu M$, $[AO7]_0 = 100\ \mu M$, and $[Cr_2O_7^{2-}]_0 = 100\ \mu M$.

of AO7 in the ternary solution was not enhanced at all by the presence of POM as shown in Fig. 5. In addition, the reduction of Cr(VI) was almost completely inhibited in the AO7/Cr(VI)/POM solution. That is, the electron transfer-mediating role of POM does not seem to work at all for the anionic dye. Since all three components involved (SiW_{12}^{4-}, AO7, and Cr(VI)) are anions in this case, their mutual electrostatic repulsion in the ternary system seems to be much stronger than that in the binary AO7/Cr(VI) system. That is, the photo-induced electron transfer from AO7 to Cr(VI) is inhibited by the presence of POM anions. In a similar context, Chen et al. have also reported that cationic dyes were degraded in the visible light-illuminated solution of SiW_{12}^{4-} whereas the degradation of an anionic dye (tetraethylsulforhodamine) was inhibited because anionic dyes scarcely interact with SiW_{12}^{4-} [17]. Therefore, the synergic effect in the simultaneous conversion in the dye/Cr(VI)/POM solution is expected only with the cationic dyes.

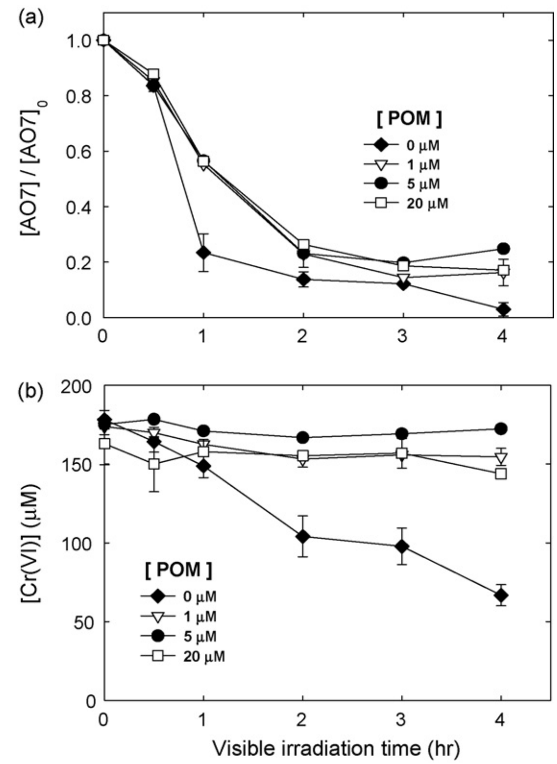

Fig. 5. Effect of SiW_{12}^{4-} concentration on the conversion of (a) AO7 and (b) Cr(VI) in the AO7/Cr(VI)/POM solution under visible light. The experimental condition was air-equilibrated, pH_i 3.0, $[AO7]_0 = 100\ \mu M$, $[Cr_2O_7^{2-}]_0 = 100\ \mu M$, and $\lambda > 420$ nm.

3.3. Mechanism of dye degradation and Cr(VI) reduction

The above results clearly show that the dye degradation rate in the ternary solution (dye/Cr(VI)/POM) was enhanced compared with that in the binary solution (dye/POM). It should be also noted that the degradation mechanism may change in the ternary system. Chen et al. reported that RhB in the visible light-illuminated solution of SiW_{12}^{4-} is degraded mainly via *N*-de-ethylation path with hypsochromic shift of the maximum absorption band whereas the cleavage of the chromophoric ring structure predominates in the visible-illuminated RhB/TiO_2 suspension [17].

To probe into the degradation mechanism, we monitored the degradation of RhB by fluorescence spectroscopy. Fig. 6 shows that the evolving fluorescence spectra of RhB in the irradiated binary RhB/POM solution were different from those in the ternary RhB/Cr(VI)/POM solution. In the presence of Cr(VI), hypsochromic shift of the emission band is more prominent. RhB and Rh-110 (a fully *N*-de-ethylated form of RhB) generate strong fluorescence bands centered at 573 nm and 520 nm, respectively [20]. More *N*-de-ethylated intermediates were produced in RhB/Cr(VI)/POM than in RhB/POM solution. This observation indicates that the presence of Cr(VI) not only changes the kinetics but also the mechanism of the dye degradation. This is speculated that fewer reactive oxygen species (ROS) is generated in the presence of Cr(VI). As illustrated in Scheme 1, Cr(VI) and O_2 are competing electron acceptors and the generation of ROS (such as $O_2^{-\bullet}$ and H_2O_2) should be hindered in the presence of Cr(VI). Since ROS attack should play a significant role in the overall dye conversion mechanism, the reduced production of ROS in the presence of Cr(VI) should influence the dye degradation mechanism. To confirm the role of O_2, the

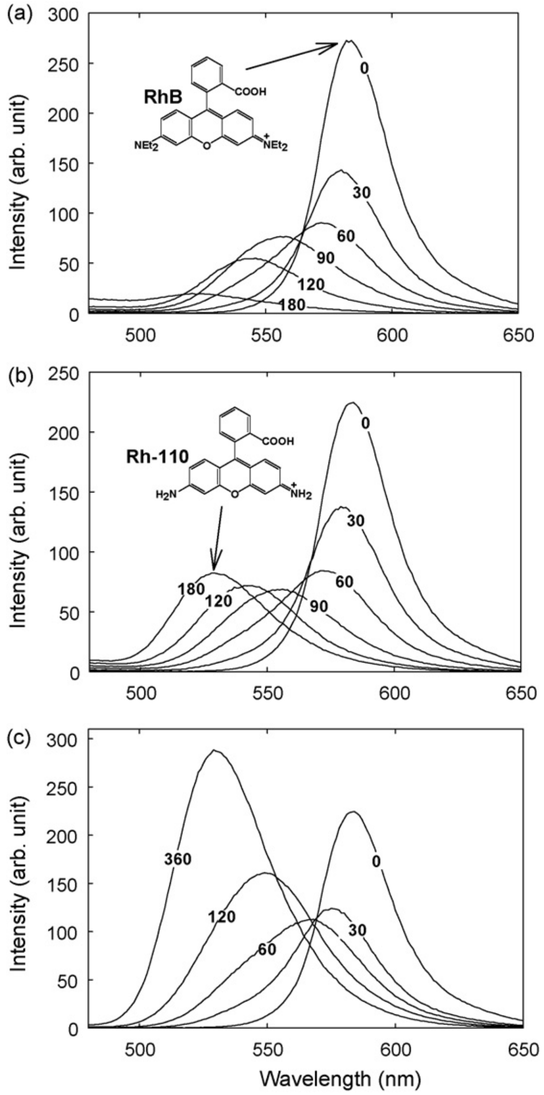

Fig. 6. The evolution of the fluorescence spectra of RhB (excited at 355 nm) in the irradiated solution of (a) RhB/POM (air), (b) RhB/Cr(VI)/POM (air), and (c) RhB/Cr(VI)/POM (N_2). The numbers indicate the irradiation time (min). The structures of RhB and Rh-110 and the corresponding emission bands are indicated. The experimental condition was air or N_2 equilibrated, pH_i 3.0, $[RhB]_0 = 20\ \mu M$, $[Cr_2O_7^{2-}]_0 = 30\ \mu M$, $[SiW_{12}^{4-}]_0 = 2\ \mu M$, and $\lambda > 420$ nm.

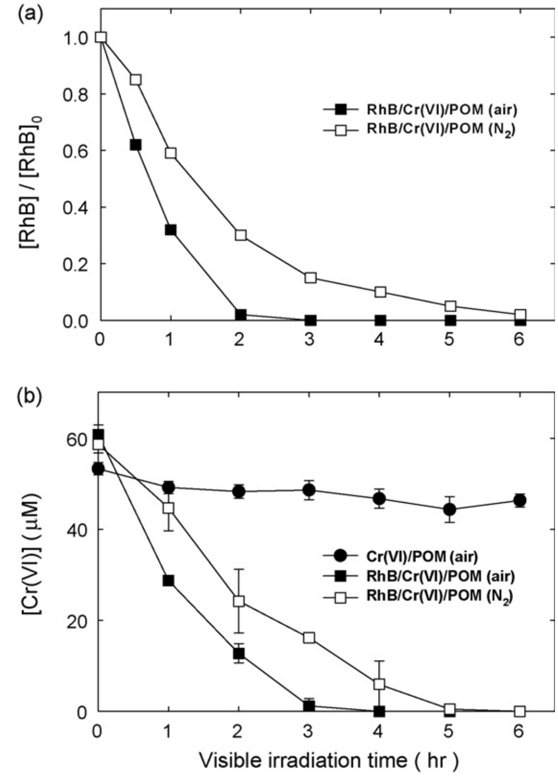

Fig. 8. The photoconversion of (a) RhB and (b) Cr(VI) in the presence or absence of dissolved oxygen under visible illumination. pH_i 3.0, $[RhB]_0 = 20\ \mu M$, $[Cr_2O_7^{2-}]_0 = 30\ \mu M$, $[SiW_{12}^{4-}]_0 = 2\ \mu M$, and $\lambda > 420$ nm.

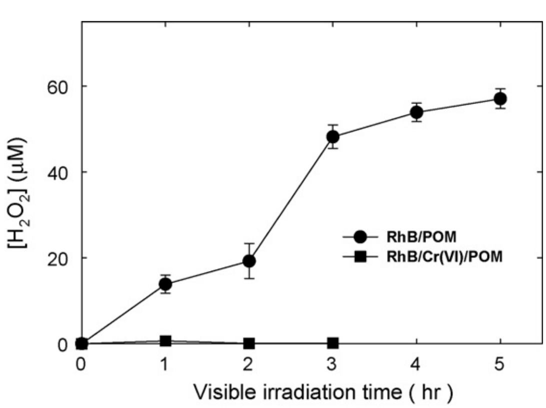

Fig. 7. H_2O_2 production from the visible-illuminated RhB/POM and RhB/Cr(VI)/POM solution. The experimental condition was air-equilibrated, pH_i 3.0, $[RhB]_0 = 20\ \mu M$, $[Cr_2O_7^{2-}]_0 = 30\ \mu M$, $[SiW_{12}^{4-}]_0 = 2\ \mu M$, and $\lambda > 420$ nm.

degradation of RhB in the ternary solution was carried out in the N_2-saturated condition. Fig. 6c shows that the production of *N*-de-ethylated intermediates was even more enhanced and RhB was almost completely de-ethylated in 6 h irradiation. With ROS production absent, the *N*-de-ethylation is strongly favored. In addition, the *in situ* production of H_2O_2 in the illuminated solution was compared between the binary and ternary system in Fig. 7. The production of H_2O_2 was significant in the RhB/POM solution but was negligible in the RhB/Cr(VI)/POM solution. This also indicates that Cr(VI) is a more efficient electron acceptor than O_2 and its presence inhibits the generation of ROS. However, despite the fact that Cr(VI) and O_2 compete for electrons, the conversion of Cr(VI) as well as RhB was moderately faster in the presence of O_2 as shown in Fig. 8. A plausible explanation for this is that *in situ* generated H_2O_2 further reduces Cr(VI).

$$2SiW_{12}^{5-} + O_2 + 2H^+ \rightarrow 2SiW_{12}^{4-} + H_2O_2 \qquad (3)$$

$$3HCrO_4^- + 3H_2O_2 + 8H^+ \rightarrow 3Cr^{3+} + 3O_2 + 4H_2O \qquad (4)$$

The enhanced photoreduction of Cr(VI) in the presence of O_2 was also observed in the studies of UV-illuminated ZnO/Cr(VI) system [21,22] and the visible-illuminated dye/Cr(VI)/TiO_2 system [18], which was ascribed to the role of reactions (3) and (4).

The simultaneous conversion of RhB and Cr(VI) in SiW_{12}^{4-} solution was also carried out under UV plus visible irradiation ($\lambda > 300$ nm) that mimics the solar irradiation. In the presence of UV light, POM as well as RhB should be excited and the overall electron transfer process is more complex. Nevertheless, the general photochemical behaviors observed

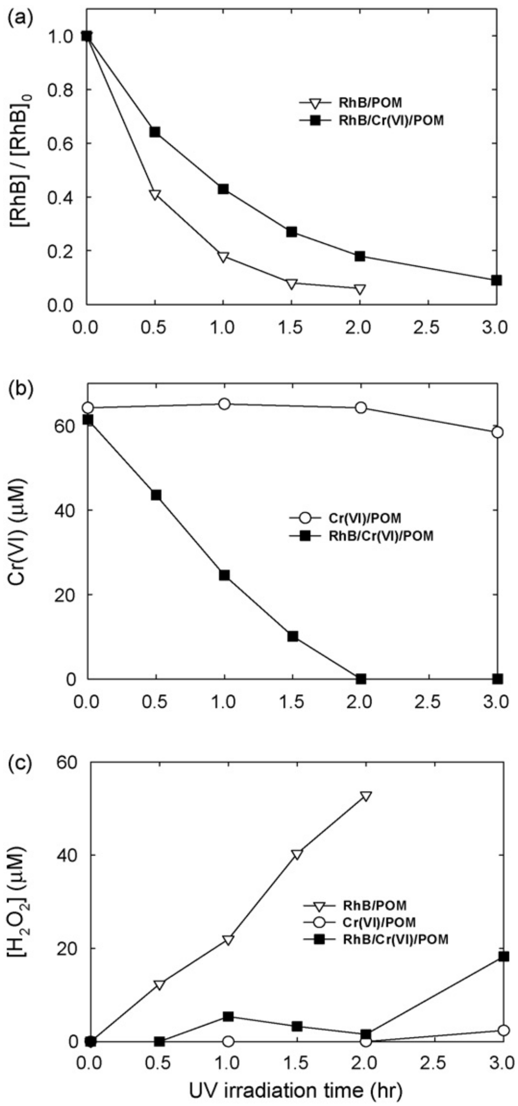

Fig. 9. The photoconversion of (a) RhB and (b) Cr(VI) under UV illumination. (c) H_2O_2 production from the UV-illuminated RhB/POM, Cr(VI)/POM and RhB/Cr(VI)/POM solution. The experimental condition was air-equilibrated, pH$_i$ 3.0, $[RhB]_0$ = 20 μM, $[Cr_2O_7^{2-}]_0$ = 30 μM, $[SiW_{12}^{4-}]_0$ = 2 μM, and $\lambda > 300$ nm.

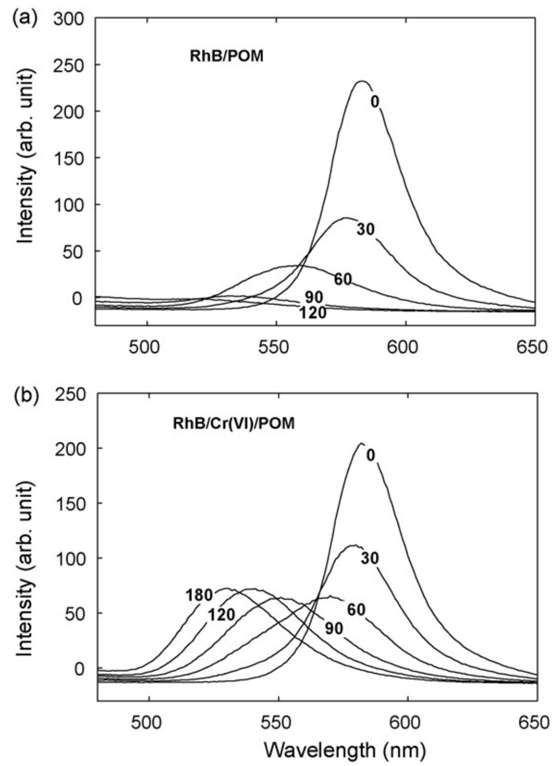

Fig. 10. The evolution of the fluorescence spectra of RhB (excited at 355 nm) in the irradiated solution of (a) RhB/POM, (b) RhB/Cr(VI)/POM. The numbers indicate the irradiation time (min). The experimental condition was air-equilibrated, pH$_i$ 3.0, $[RhB]_0$ = 20 μM, $[Cr_2O_7^{2-}]_0$ = 30 μM, $[SiW_{12}^{4-}]_0$ = 2 μM, and $\lambda > 300$ nm.

under $\lambda > 300$ nm irradiation were similar to those observed under visible light ($\lambda > 420$ nm). The results are shown in Fig. 9. Cr(VI) could not be converted at all in the Cr(VI)/POM solution even under $\lambda > 300$ nm whereas its reductive transformation was highly enhanced in the RhB/Cr(VI)/POM solution. The *in situ* production of H_2O_2 in the UV-illuminated RhB/Cr(VI)/POM solution was significantly hindered as long as Cr(VI) was present whereas the production of H_2O_2 in the RhB/POM solution increased up to 50 μM in 2 h of UV irradiation, which is similarly compared with the visible light system (Fig. 7). The evolution of the fluorescence spectra under UV plus visible irradiation showed that the *N*-de-ethylation with the hypsochromic shift of RhB absorption band was more dominant in the presence of Cr(VI) (Fig. 10), which is also similarly compared with the visible light system (Fig. 6). Therefore, the synergic effect observed in the visible-illuminated dye/Cr(VI)/POM system might be applied to the solar illumination (UV plus visible) condition as well.

4. Conclusions

POM has been frequently studied as a homogeneous photocatalyst. Although POM is inactive under visible light, it can be sensitized by dyes as semiconductor photocatalyst (e.g., TiO_2) is. The LUMO of POM plays the role of electron transfer mediator as the semiconductor conduction band does in the dye-sensitization process. With taking advantage of this dye-sensitization process of POM, simultaneous conversion of dye and hexavalent chromium (Cr(VI)) in visible light-illuminated POM solution was successfully demonstrated in this study. The simultaneous conversion of cationic dye and anionic Cr(VI) was synergically enhanced in the presence of POM, which indicate that POM successfully plays the role of the electron transfer catalyst from the excited cationic dye to Cr(VI).

Acknowledgments

This work was supported by the KOSEF Nano R&D program (Grant No. 2005-02234), the SRC/ERC program of MOST/KOSEF (Grant No. R11-2000-070-06004-0), and BK21 program.

References

[1] E. Androulaki, A. Hiskia, D. Dimotikali, C. Minero, P. Calza, E. Pelizzetti, E. Papaconstantinou, Environ. Sci. Technol. 34 (2000) 2024–2028.
[2] A. Hiskia, A. Mylonas, E. Papaconstantinou, Chem. Soc. Rev. 30 (2001) 62–69.
[3] S. Kim, H. Park, W. Choi, J. Phys. Chem. B 108 (2004) 6402–6411.
[4] R.R. Ozer, J.L. Ferry, Environ. Sci. Technol. 35 (2001) 3242–3246.
[5] A. Ioannidis, E. Papaconstantinou, Inorg. Chem. 24 (1985) 439–441.
[6] A. Troupis, A. Hiskia, E. Papaconstantinou, New. J. Chem. 25 (2001) 361–363.
[7] A. Troupis, A. Hiskia, E. Papaconstantinou, Angew. Chem. Int. Ed. 41 (2002) 1911–1914.
[8] M. Hu, Y. Xu, Chemosphere 54 (2004) 431–434.

[9] A. Troupis, A. Hiskia, E. Papaconstantinou, Environ. Sci. Technol. 36 (2002) 5355–5362.
[10] A. Gkika, A. Troupis, A. Hiskia, E. Papaconstantinou, Environ. Sci. Technol. 39 (2005) 4242–4248.
[11] A. Gkika, A. Troupis, A. Hiskia, E. Papaconstantinou, Appl. Catal. B: Environ. 62 (2006) 28–34.
[12] C. Nasr, K. Vinodgopal, L. Fisher, S. Hotchandani, A.K. Chattopadhyay, P.V. Kamat, J. Phys. Chem. 20 (1996) 8436–8442.
[13] T. Wu, T. Lin, J. Zhao, H. Hidaka, N. Serpone, Environ. Sci. Technol. 33 (1999) 1379–1387.
[14] Y. Cho, W. Choi, C.H. Lee, T. Hyeon, H.I. Lee, Environ. Sci. Technol. 35 (2001) 966–970.
[15] C. Chen, W. Zhao, J. Li, J. Zhao, H. Hidaka, N. Serpone, Environ. Sci. Technol. 36 (2002) 3604–3611.
[16] E. Bae, W. Choi, Environ. Sci. Technol. 37 (2003) 147–152.
[17] C. Chen, W. Zhao, P. Lei, J. Zhao, N. Serpone, Chem. Eur. J. 10 (2004) 1956–1965.
[18] H. Kyung, J. Lee, W. Choi, Environ. Sci. Technol. 39 (2005) 2376–2382.
[19] H. Lee, W. Choi, Environ. Sci. Technol. 36 (2002) 3872–3878.
[20] H. Park, W. Choi, J. Phys. Chem. B 109 (2005) 11667–11674.
[21] L.B. Khalil, W.E. Mourad, M.W. Rophael, Appl. Catal. B: Environ. 17 (1998) 267–273.
[22] J. Domenech, J. Munoz, Electrochim. Acta 32 (1987) 1383–1386.